# Alveolar macrophages develop from fetal monocytes that differentiate into long-lived cells in the first week of life via GM-CSF

Martin Guilliams,[1,2,3] Ismé De Kleer,[1,2,4] Sandrine Henri,[3] Sijranke Post,[1,2] Leen Vanhoutte,[1,2,5] Sofie De Prijck,[1,2] Kim Deswarte,[1,2] Bernard Malissen,[3] Hamida Hammad,[1,2] and Bart N. Lambrecht[1,2,4]

[1]Laboratory of Immunoregulation and Mucosal Immunology, VIB Inflammation Research Center, 9050 Ghent, Belgium
[2]Department of Pulmonary Medicine, Ghent University, Ghent, 9000, Belgium
[3]Centre d'Immunologie de Marseille-Luminy (CIML), Institut National de la Santé et de la Recherche Médicale U1104, Centre National de la Recherche Scientifique UMR7280, Aix Marseille Université, 13288 Marseille, France
[4]Department of Pulmonary Medicine, Erasmus University Medical Center, 3015 Rotterdam, The Netherlands
[5]Department of Clinical Genetics, Ghent University Hospital, 9000 Ghent, Belgium

**Tissue-resident macrophages can develop from circulating adult monocytes or from primitive yolk sac–derived macrophages. The precise ontogeny of alveolar macrophages (AMFs) is unknown. By performing BrdU labeling and parabiosis experiments in adult mice, we found that circulating monocytes contributed minimally to the steady-state AMF pool. Mature AMFs were undetectable before birth and only fully colonized the alveolar space by 3 d after birth. Before birth, F4/80$^{hi}$CD11b$^{lo}$ primitive macrophages and Ly6C$^{hi}$CD11b$^{hi}$ fetal monocytes sequentially colonized the developing lung around E12.5 and E16.5, respectively. The first signs of AMF differentiation appeared around the saccular stage of lung development (E18.5). Adoptive transfer identified fetal monocytes, and not primitive macrophages, as the main precursors of AMFs. Fetal monocytes transferred to the lung of neonatal mice acquired an AMF phenotype via defined developmental stages over the course of one week, and persisted for at least three months. Early AMF commitment from fetal monocytes was absent in GM-CSF–deficient mice, whereas short-term perinatal intrapulmonary GM-CSF therapy rescued AMF development for weeks, although the resulting AMFs displayed an immature phenotype. This demonstrates that tissue-resident macrophages can also develop from fetal monocytes that adopt a stable phenotype shortly after birth in response to instructive cytokines, and then self-maintain throughout life.**

CORRESPONDENCE
Martin Guilliams:
martin.guilliams@ugent.be

Abbreviations used: AMF, alveolar MF; BAL, bronchoalveolar lavage; DOB, date of birth; DT, diphtheria toxin; DTR, DT receptor; GM-CSF, granulocyte-MF colony-stimulating factor; GM-CSF-R, GM-CSF receptor (CD116); LC, Langerhans cell; MF, macrophage; PND, postnatal day; rGM-CSF, recombinant GM-CSF; SEM, scanning electron microscopy.

Alveolar macrophages (AMF) are the prototypical MFs of the lung that have important functions in lung development, surfactant homeostasis, pathogen clearance, and immune homeostasis (Lambrecht, 2006). Among tissue resident MFs, AMFs have a peculiar phenotype in that they are highly autofluorescent, express low levels of the phagocytic receptor CD11b, yet high levels of the integrin CD11c, and high levels of the lectin SiglecF, allowing them to be easily recognized among other myeloid cells of the lung (Gautier et al., 2012b; Misharin et al., 2013). For a long time, AMFs were considered the prototypical cells belonging to the unified mononuclear phagocyte system (MPS), a family of tissue-resident MFs proposed to derive from circulating BM-derived monocytes that seed the various tissues in the steady state and continuously differentiate locally into tissue-resident MFs (van Furth and Cohn, 1968; Geissmann et al., 2010). The MPS concept with the circulating monocyte as the central precursor to all tissue MFs was based on in vivo adult monocyte transfer experiments (Geissmann et al., 2003), in vivo thymidine-(3)H labeling experiments (van Furth and Cohn, 1968), and the study of irradiation chimeras (Virolainen, 1968). Depletion of AMFs using intratracheal administration

M. Guilliams, I. De Kleer, and S. Henri contributed equally to this paper.



The Rockefeller University Press $30.00
J. Exp. Med. 2013 Vol. 210 No. 10 1977-1992
www.jem.org/cgi/doi/10.1084/jem.20131199



The Journal of Experimental Medicine

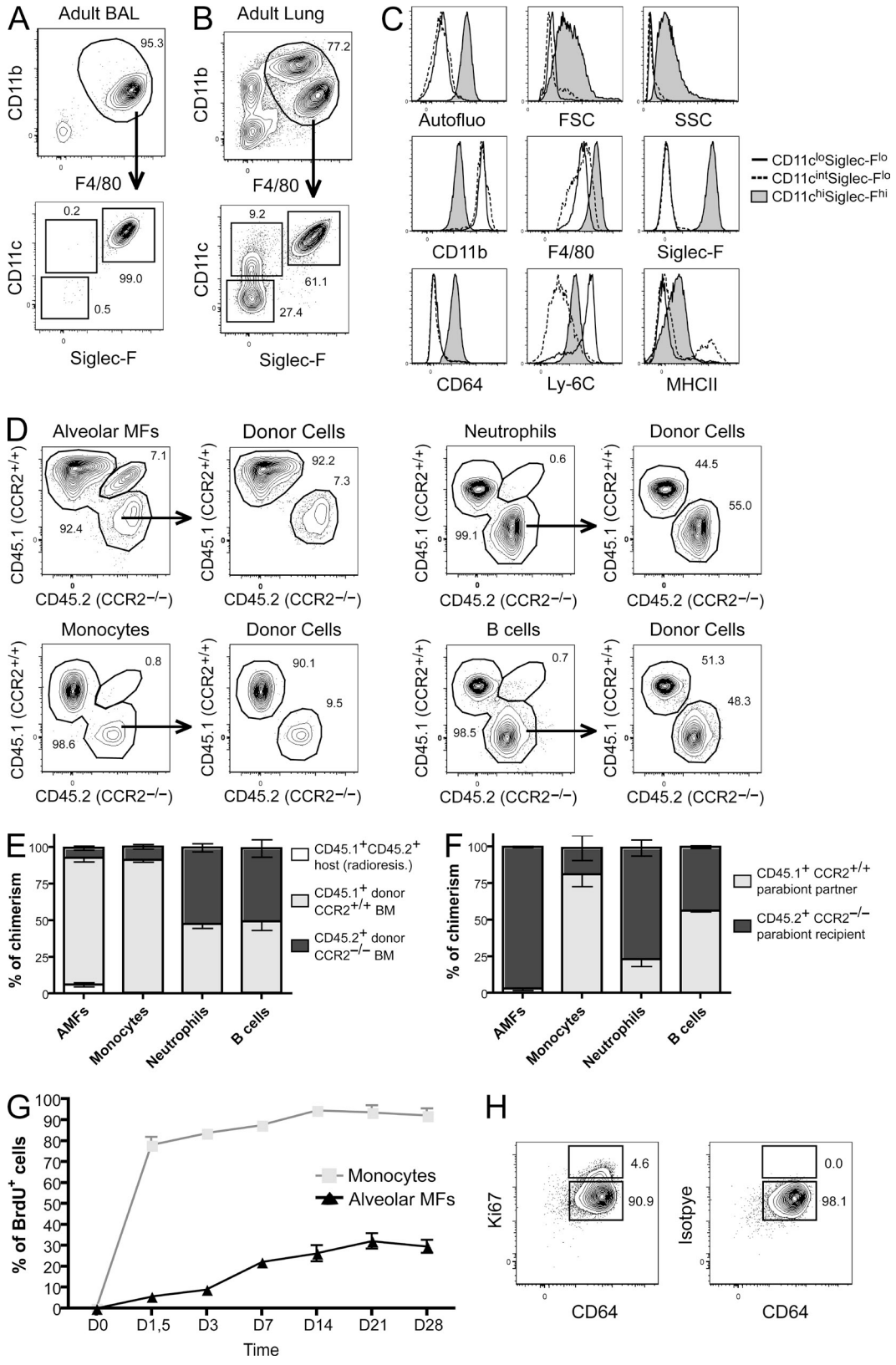


**Figure 1. AMFs self-maintain locally with minimal contribution from circulating hematopoietic precursors.** BAL (A) and total lung (B) were harvested from adult mice and stained for CD11b, F4/80, SiglecF, CD64, Ly-6C, and MHCII and evaluated for autofluorescence, FSC, and SSC profile (C). (D) CD45.1$^+$CD45.2$^+$ mice were lethally irradiated and reconstituted with equal amounts of CD45.1$^+$ WT and CD45.2$^+$CCR2$^{-/-}$ BM cells. Radio-resistant cells,

of diphtheria toxin (DT) to CD11c-DT receptor (DTR) mice followed by transfer of monocytes demonstrated that adult BM-derived monocytes can indeed differentiate into AMFs in vivo (Landsman and Jung, 2007). However, genetic fate mapping experiments using hematopoietic (*Myb*) or monocyte-based (*Cx3cr1*) fate mapping gene promoters found these cells to be only partially (Schulz et al., 2012) or not at all (Yona et al., 2013) of adult hematopoietic or monocytic origin, which was hard to reconcile with the MPS concept. Part of the confusion on the precise origin of AMFs also stems from the fact that these cells are long lived and relatively radioresistant depending of the radiation dose, complicating the interpretation of radiation chimeric experiments. Therefore, whereas some proposed a monocytic origin for AMF (Godleski and Brain, 1972; van oud Alblas and van Furth, 1979; Kennedy and Abkowitz, 1997; Kennedy and Abkowitz, 1998) others proposed that AMFs would be mainly long-lived, self-renewing cells (Tarling et al., 1987; Murphy et al., 2008).

The MPS paradigm with the circulating monocyte as the central replenisher of all tissue MFs has also been challenged recently by the observation that MFs appear in embryonic tissues before the development of monocytes, making it hard to envisage a precursor-product relationship for monocytes and MFs (Takahashi et al., 1989; Ginhoux et al., 2010; Hoeffel et al., 2012; Schulz et al., 2012). Supporting the idea of primitive MF progenitors seeding the tissues, some tissue-resident MFs like microglia (Ajami et al., 2007, 2011) and Kupffer cells (Bouwens et al., 1986a,b; Yamamoto et al., 1996) were found not to derive from circulating hematopoietic precursors but to be long-lived, self-renewing cells. Using genetic fate mapping, microglia was found to be derived from fetal yolk sac MFs that seed the brain before birth and then maintain locally without any input from adult hematopoietic precursors or circulating monocytes (Ginhoux et al., 2010). When first proposed, the primitive origin of microglia was thought to represent an exception to the MPS concept, as microglia populate a cellular niche that is normally not accessible to hematopoietic precursors because of the blood–brain barrier that closes shortly before birth. However, subsequent studies found that most tissue-resident MFs, including Kupffer cells, splenic MFs, peritoneal MFs, and kidney MFs, are not of adult hematopoietic origin in the steady state (Schulz et al., 2012; Yona et al., 2013), leading to the generalization that these cells may also develop directly from yolk sac–derived fetal MFs (Gomez Perdiguero et al., 2013).

Given the controversies surrounding the development of AMFs and these recent developments on the origin of other tissue-resident MFs, we readdressed the origin of AMFs and found that these cells are not replenished continuously from adult monocytes, but instead derive from fetal monocytes that seed the lung before birth and develop into long-lived CD11c$^{hi}$, SiglecF$^{hi}$ AMFs shortly after birth in response to an instructive signal provided by granulocyte-MF colony-stimulating factor (GM-CSF). In GM-CSF–deficient mice, a few days of perinatal cytokine therapy were able to restore AMF development for weeks. Differentiation of AMFs from fetal monocytes starts around the time alveoli develop (E18.5), and is completed over the course of 1 wk. These findings reconcile previous controversies on AMF ontology and provide new clues to the developmental origin of this unique MF population resident in the lung compartment from fetal monocytes.

## RESULTS

### Identification of lung mononuclear cells

We first addressed if AMFs derived from a circulating precursor population. To precisely define the different mononuclear cells of the lung, we performed 10-color flow cytometry on bronchoalveolar lavage (BAL) fluid and total lung cell suspensions after blood was rinsed from the pulmonary circulation. First, neutrophils (Ly-6G$^{hi}$CD11b$^{hi}$CD64$^{lo}$Ly-6C$^{hi}$cells), eosinophils (SiglecF$^{hi}$CD11b$^{hi}$CD64$^{lo}$Ly-6C$^{int}$ cells), T cells (CD3$^{hi}$ CD11b$^{lo}$CD64$^{lo}$ cells), and B cells (CD19$^{hi}$CD11b$^{lo}$CD64$^{lo}$ cells) were outgated (unpublished data). Second, not to miss any mononuclear cells, we first gated lung cells on a broad mononuclear gate consisting of F4/80$^{+}$ and CD11b$^{+}$ cells. AMFs have a distinct phenotype among tissue-resident MFs and can be unequivocally identified within the F4/80$^{+}$CD11b$^{+}$ gate as SiglecF$^{hi}$CD11c$^{hi}$ cells in the BAL fluid (Fig. 1 A; Gautier et al., 2012b). The same population could also be found in total cell suspensions of lung tissue (Fig. 1 B), when BAL fluid was not collected before homogenization. In lung tissue, the F4/80$^{+}$CD11b$^{+}$ gate contained a second population of CD11b$^{hi}$F4/80$^{int}$ cells that were further subdivided into CD11c$^{lo}$SiglecF$^{lo}$ cells and CD11c$^{int}$SiglecF$^{lo}$ cells. Using this gating strategy, SiglecF$^{hi}$CD11c$^{hi}$ cells were large (FSC$^{hi}$), and granular (SSC$^{hi}$) highly autofluorescent cells (Fig. 1 C), typical of alveolar MFs (Vermaelen and Pauwels, 2004). We next measured the expression of various markers on these three identified populations of lung cells (Fig. 1 C). The universal MF marker CD64 was expressed highly on SiglecF$^{hi}$ CD11c$^{hi}$ AMFs, but not on the other two populations. The marker Ly-6C is highly expressed on circulating monocytes, but less on monocytes that patrol the blood vessels (Geissmann et al., 2003). The CD11b$^{hi}$F4/80$^{int}$CD11c$^{lo}$SiglecF$^{lo}$ population expressed

distinguished as CD45.1$^{+}$CD45.2$^{+}$ cells, were gated out, and the remaining BM-derived cells of the indicated populations were analyzed for their ratio of CD45.1$^{+}$ WT and CD45.2$^{+}$CCR2$^{-/-}$ cells. (E) Summary data from five independent chimeric mice. (F) Parabiotic mice were generated by suturing together CD45.1$^{+}$ WT and CD45.2$^{+}$CCR2$^{-/-}$ mice. The percentage of cells of CD45.1$^{+}$ WT donor origin was determined in B cells, neutrophils, and monocytes in the blood and AMFs in the lungs of the CD45.2$^{+}$CCR2$^{-/-}$ parabionts. (G) Adult C57BL/6 mice received BrdU continuously for 28 d. Mice were sacrificed at regular intervals, and incorporation of BrdU in lung AMFs and monocytes was evaluated. (H) Adult C57BL/6 mice were sacrificed and Ki-67 expression (left) was determined in AMFs. The isotype staining is shown (right). Data represent at least three (A– E) or two (F– H) independent experiments involving at least six (E) and four (F and G) independent mice.

high levels of Ly-6C, identifying these cells as monocytes. In support, they also did not express the MF marker CD64 and were $SSC^{lo}$ and $FSC^{lo}$. The $CD11b^{hi}F4/80^{int}CD11c^{int}SiglecF^{lo}$ population was a mixed population in which some cells expressed low levels of Ly-6C (likely representing residual vessel patrolling monocytes) and ∼20% expressed high levels of MHCII (thus representing mature $CD11b^+$ cDCs). Interstitial MFs (defined as $CD11b^{hi}$, $F4/80^{hi}$, $CD11c^-$, $SiglecF^{lo}$, $MHCII^+$, $CD64^+$ cells represented <5% of cells in the $CD11b^+$ $F4/80^+$ mononuclear gate and <0.2% of lung suspension cells (dot plots not depicted).

### Adult circulating monocytes contribute to the AMF pool in irradiated mice, but not in homeostasis

Previous work supporting the fact that AMFs belong to the MPS system have studied AMF pool replenishment after whole-body irradiation, illustrating that the AMF pool can derive from an adult hematopoietic progenitor. However, it has not been formally shown that circulating monocytes constitute the main precursor of the AMF pool after irradiation, or only participate minimally to the AMF pool. To test this, congenic mice coexpressing CD45.1 and CD45.2 were lethally irradiated and reconstituted with a 1:1 mixture of BM cells isolated from $CD45.1^+$ C57BL/6 WT mice and from $CD45.2^+$ *Ccr2*$^{-/-}$ mice. These B6 (CD45.1) WT + B6 (CD45.2) *Ccr2*$^{-/-}$ → B6 (CD45.1–CD45.2) competitive chimeras were analyzed 8 wk after BM transfer. As CCR2 is critical for egress of monocytes from the BM (Serbina and Pamer, 2006), competitive chimerism allowed us to address the relative contribution of circulating monocytes to AMF replenishment after whole body irradiation. As expected, Ly-$6C^{hi}$ blood monocytes were primarily composed of $CD45.1^+CCR2^+$ donor cells, whereas neutrophils and B cells were comprised of almost equal percentages of $CD45.1^+$ and $CD45.2^+$ donor cells (Fig. 1 D, group summarized in Fig. 1 E). 8 wk after reconstitution, AMFs still contained between 5 and 10% of host-derived, radio-resistant $CD45.1^+CD45.2^+$ cells, illustrating the relative radioresistance of these cells (Fig. 1 E). The donor-derived AMFs showed CD45 chimerism identical to those of Ly-$6C^{hi}$ blood monocytes, demonstrating that upon severe depletion, AMFs derive from circulating monocytes.

We next questioned whether circulating monocytes participate to the AMF pool in the adult life when AMFs are not experimentally depleted by irradiation. We therefore performed parabiosis experiments between $CD45.1^+$ WT mice and $CD45.2^+$ *Ccr2*$^{-/-}$ mice. After 8 wk of parabiosis, we analyzed the contribution of $CD45.1^+$ WT cells within the $CD45.2^+$ *Ccr2*$^{-/-}$ mice. There was an almost even distribution of long-lived recirculating cells, and donor $CD45.1^+$ WT B lymphocytes represented 40% of circulating blood B lymphocytes of the parabiont $CD45.2^+$ *Ccr2*$^{-/-}$ partner (Fig. 1 F). However, short-lived circulating cells like neutrophils exchanged ∼20% of the cells among the parabiont partner. Such uneven distribution between parabionts likely results from the fact that neutrophils do not spend enough time in the circulation to equilibrate between the parabionts (Liu et al., 2007). Due to a defect in monocyte egress from the BM in the $CD45.2^+$ *Ccr2*$^{-/-}$ mice, donor $CD45.1^+$ WT monocyte constituted ∼80% of the monocytes in these mice. However, in our experiments AMFs achieved a much lower chimerism in parabionts with <5% of AMFs originating from the parabiotic partner. This indicates that circulating adult hematopoietic precursors only minimally participate to the AMF pool. These data are congruent with a recent report from the Merad group (Hashimoto et al., 2013).

We next sought to find evidence for the lack of monocyte contribution to the AMF pool in unmanipulated mice. We reasoned that if monocytes were precursors to AMFs, then studying BrdU incorporation kinetics should allow us to study progenitor–product relationships (Kamath et al., 2002). We exposed C57BL/6 mice continuously to BrdU in the drinking water for 4 wk after an initial i.p. injection of BrdU. As shown in Fig. 1 G, whereas almost all monocytes were rapidly BrdU labeled within 2 d, AMFs slowly accumulated 30% of BrdU incorporation after 4 wk of continuous BrdU exposure. The slow accumulation of BrdU could come from $BrdU^+$ circulating hematopoietic progenitors or from local proliferation of AMFs. We therefore evaluated the expression of the cell cycle protein Ki-67, which labels dividing and recently divided daughter cells. As shown in Fig. 1 H, a small population (<5%) of $Ki\text{-}67^+$ dividing cells could be found among AMFs, suggesting a slow local proliferation of AMFs.

To further evaluate whether circulating monocytes contribute to the AMF pool of unmanipulated mice, we transferred $2 \times 10^6$ $CD45.1^+$ Ly-$6C^{hi}$ $CD11b^{hi}$ monocytes into adult *Ccr2*$^{-/-}$ $CD45.2^+$ mice, but we could not recover any transferred monocyte developing into $SiglecF^{hi}CD11c^{hi}$ AMFs 7 d after the transfer, although we readily recovered transferred monocytes as mature intestinal MFs 7 d after transfer (not depicted; Tamoutounour et al., 2012; Bain et al., 2013).

### Alveolar MFs appear in the alveolar space during the first week of life

Microglia and Langerhans cells (LCs) derive from embryonic precursors that seed the brain and the skin before birth and maintain themselves locally throughout life (Chorro et al., 2009; Ginhoux et al., 2010; Hoeffel et al., 2012). As AMFs also did not derive from circulating monocytes and showed signs of low-grade proliferation, we next addressed the ontogeny of AMF before and after birth. Little is known about the ontogeny of the lung immune system in relation to lung development, which proceeds via a pseudoglandular stage (E9.5–E16.5), a canalicular stage (E16.5–17.5), and a saccular stage (E18.5 to postnatal day [PND] 5). During the latter stage, canaliculi develop numerous sacs that are the precursors to the alveoli. As shown in Fig. 2 A, we first measured the kinetics of $CD45^+$ leukocyte accumulation in the lung. The percentage of $CD45^+$ cells started expanding around E18, coinciding with the start of the saccular stage (Fig. 2 C). We next addressed the ontogeny of mononuclear cells (Fig. 2 B). At day E12, the major population of mononuclear cells in the $CD11b^+$ $F4/80^+$ gate consisted of $F4/80^{hi}$ $CD11b^{int}$ cells, which had an intensity of staining resembling adult mature AMFs. However, these cells

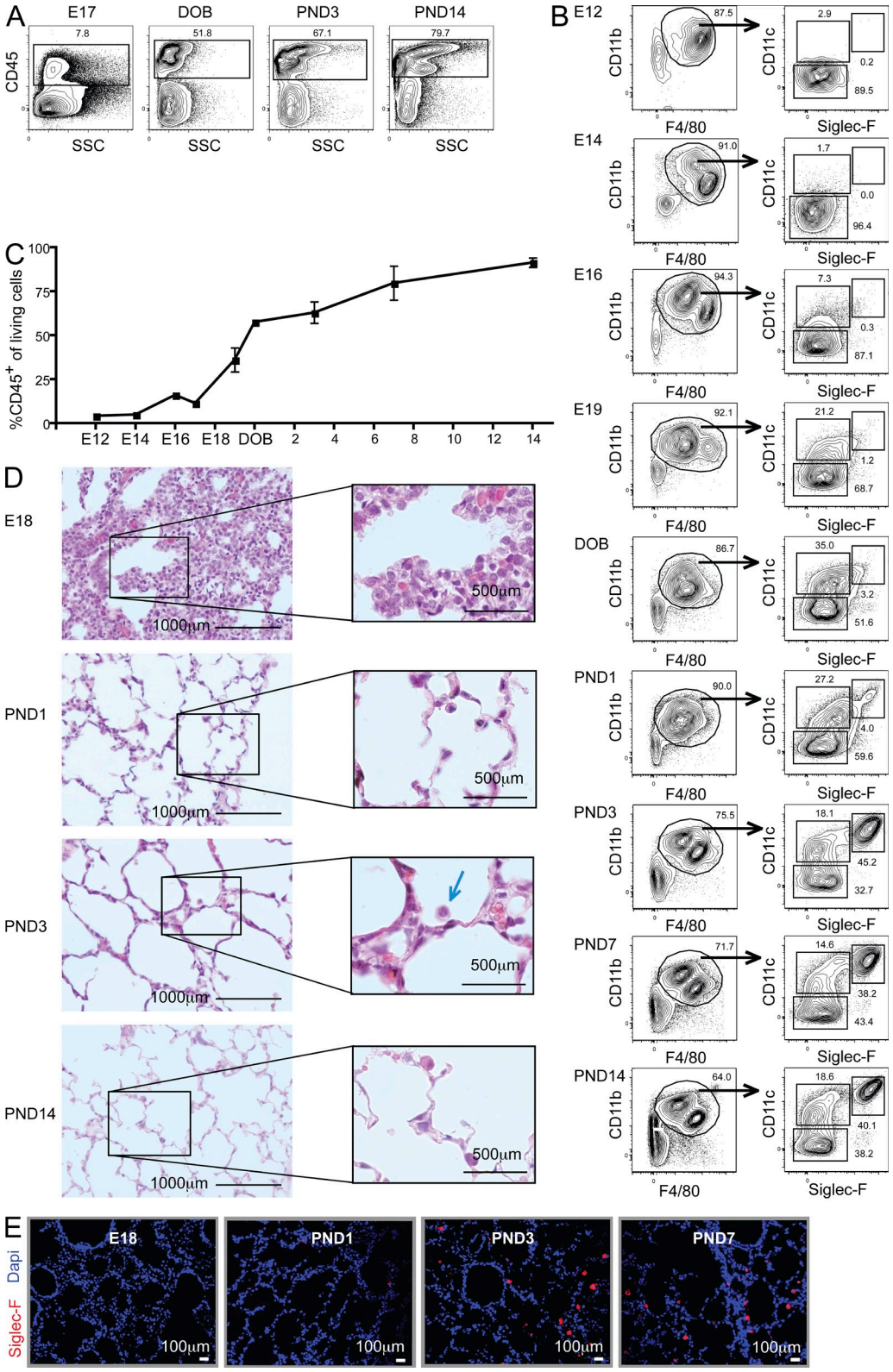


**Figure 2. Alveolar MFs appear in the alveolar space during the first week of life.** Lungs were harvested at various time points before and after (PND) the DOB. (A and C) Flow cytometry staining for CD45+ cells. (B) CD11b+F4/80+ myeloid cells were gated and analyzed for CD11c and SiglecF expression. (D) Paraffin lung sections stained with hematoxylin. (E) Cryosection of lungs stained with DAPI (blue) and SiglecF (red). Data in A–E represent at least two independent experiments involving at least three independent mice per time point.

were completely negative for SiglecF and CD11c. They were most reminiscent of the phenotype of primitive MFs that arise at E9 and E12 from the yolk sac, and are also CD11b$^{int}$ F4/80$^{hi}$ (unpublished data). Progressively, the mononuclear gate became replete with a second F4/80$^{int}$ CD11b$^{hi}$ population, and there was a gradual increase in the cells expressing intermediate levels of CD11c. However, before birth, the mononuclear gate was completely devoid of SiglecF$^{hi}$CD11c$^{hi}$ AMFs. Around the date of birth (DOB), the mononuclear gate was in transition, and it was no longer possible to clearly discern F4/80$^{hi}$ from F4/80$^{int}$ cells. There was a marked increase in CD11c$^{int}$ cells. Mature SiglecF$^{hi}$CD11c$^{hi}$ AMFs only appeared between PND1 and PND3, when a predominant population of F4/80$^{hi}$ cells was again apparent in the mononuclear gate. Interestingly, this time point coincided with the first appearance of large mononuclear cells in the alveolar space (Fig. 2 D). Mature SiglecF-expressing AMFs were first found in the lung septa at PND1, and accumulated in the alveolar lumen at PND3 (Fig. 2 E). When we studied lungs before birth, the developing airspaces were completely devoid of mononuclear cells (Fig. 2 D and E). Therefore, bona fide SiglecF$^{hi}$CD11c$^{hi}$ AMFs only appear in the alveolar space during the first days of life.

### Fetal MFs, fetal monocytes, preAMFs, and mature AMFs appear in consecutive waves during lung development

The kinetic analysis of lung mononuclear cells and AMF ontology demonstrated that the phenotype of lung mononuclear cells was highly dynamic, and composed of cells resembling fetal monocytes, fetal MFs, and immature AMFs, with significant overlap in expression of marker sets. We therefore studied the phenotype of mononuclear cells in greater detail, again using the basic mononuclear gate and three populations CD11c$^{hi}$SiglecF$^{hi}$, CD11c$^{int}$SiglecF$^{lo}$, and CD11c$^{lo}$SiglecF$^{lo}$ as the starting gate, just like in adult mice (Fig. 3 A). As illustrated in Fig. 3 B for the E17 time point, most mononuclear cells were SiglecF$^{lo}$CD11c$^{lo}$ cells that could be readily subdivided into CD11b$^{int}$F4/80$^{hi}$ and CD11b$^{hi}$F4/80$^{int}$ cells. These cells also differentially expressed the monocytic marker Ly-6C (Fig. 3 B). Ly-6C$^{lo}$ F4/80$^{hi}$ cells highly expressed CD64 (Fig. 3 C), a core MF marker (Gautier et al., 2012b; Tamoutounour et al., 2012), showed a typical MF morphology on SEM (Fig. 3 D), and adhered to plastic in vitro. On the contrary, Ly-6C$^{hi}$F4/80$^{int}$ did not express CD64 and had the typical monocytic FSC$^{lo}$SSC$^{lo}$ profile (not depicted) and displayed a nonadherent monocytic morphology on scanning electron microscopy (SEM; Fig. 3 D), thus constituting fetal monocytes. Given their kinetic appearance and resemblance to fetal liver monocytes (not depicted), these were likely derived from the liver, the major hematopoietic organ at this time period of development. From E18 onwards, but culminating around DOB (Fig. 3, A–C, second column), a predominant population of SiglecF$^{lo}$CD11c$^{int}$ cells appeared. These cells were mainly CD11b$^{hi}$F4/80$^{int}$ and were Ly-6C$^{int}$ and expressed intermediate levels of CD64. On SEM, these cells were larger and more granular like AMFs, but did not adhere well to plastic (Fig. 3 D, preAMF). Very few MHCII$^{+}$ DCs were found in this gate (data not shown). At DOB, the SiglecF$^{lo}$CD11c$^{lo}$ cells still contained some Ly-6C$^{lo}$F4/80$^{hi}$ fetal MFs, but Ly-6C$^{hi}$F4/80$^{int}$ fetal monocytes were the predominant population. Within the SiglecF$^{lo}$CD11c$^{lo}$ cells, some monocytes had already lost Ly-6C, a common feature of monocytes differentiating into mature MFs or DCs (Tamoutounour et al., 2012; Plantinga et al., 2013). Between PND1 and PND3, SiglecF$^{hi}$CD11c$^{hi}$ cells appeared very suddenly, and these were Ly-6C$^{lo}$F4/80$^{hi}$ cells, like adult AMFs. The SiglecF$^{lo}$CD11c$^{int}$ cells contained more MHCII DCs (not depicted), but still contained many mononuclear cells that were losing Ly-6C. At PND3 (Fig. 3, A–C, third column), the SiglecF$^{lo}$CD11c$^{lo}$ fraction hardly contained any F4/80$^{hi}$ fetal MFs anymore. At PND14 (Fig. 3, A–C, fourth column), the ensemble of lung mononuclear cell types resembled the adult state, and the CD11c$^{int}$ population had lower mean fluorescence expression of SiglecF. In Fig. 3 E, the relative distribution of all these cell populations is plotted against time. The appearance of mature AMFs at PND3 was preceded by a surge in SiglecF$^{lo}$CD11c$^{int}$ CD64$^{int}$ cells that looked like immature AMFs on SEM. We will therefore call this population preAMFs.

### Fetal monocytes give rise to self-maintaining AMFs through a preAMF intermediate step

To verify whether fetal monocytes or fetal MFs are the direct precursors to AMFs, we designed a competitive transfer experiment (Fig. 4). CD45.1 fetal MFs and CD45.2 monocytes were isolated from E17 lungs and transferred together in a 1:1 ratio i.n.) into CD45.1$^{+}$ CD45.2$^{+}$ mice on their DOB, i.e., when the AMF niche is still empty. 7 d after transfer, the fate of the donor cells was evaluated. Whereas at day 7, most of the AMFs were of host CD45.1$^{+}$CD45.2$^{+}$ phenotype in these nonirradiated mice (Fig. 4 A), the fate of donor cells could clearly be defined. As shown in Fig. 4 (A and B), transferred AMFs were significantly more derived from fetal monocyte–derived MFs than from fetal MFs. Similar results were found when the congenic donor pair was switched over (i.e. when fetal monocytes were CD45.1 and fetal MFs were CD45.2) or when the recipient mice were analyzed at 6 weeks after transfer (unpublished data) instead of 7 days after transfer (Fig. 4, A and B). A similar setup also allowed us to follow the differentiation of developing AMFs from adoptively transferred fetal monocytes. Therefore, we i.n. transferred fetal CD45.1$^{+}$ monocytes into CD45.2$^{+}$ mice on DOB and checked the phenotypic changes of the cells in the following days and weeks. Strikingly, transferred CD45.1 cells could be found up to 11 wk after transfer (Fig. 4 C). Fetal monocytes gradually increased expression of CD11c, SiglecF, F4/80, and CD64 levels, while down-regulating first Ly-6C and then CD11b, going through a Ly-6C$^{int}$CD11b$^{hi}$F4/80$^{int}$Ly-6C$^{int}$CD64$^{int}$ intermediate stage, essentially validating these cells as preAMFs. The kinetic of the differentiation of the transferred monocytes fits a developmental scheme that would go from fetal monocytes over preAMFs to mature AMFs within 6 to 7 d, which was also seen in Fig. 3 E. We could still trace back AMF originating from transferred monocytes 3 mo after transfer. Moreover, within one transfer experiment, the percentage of donor-derived

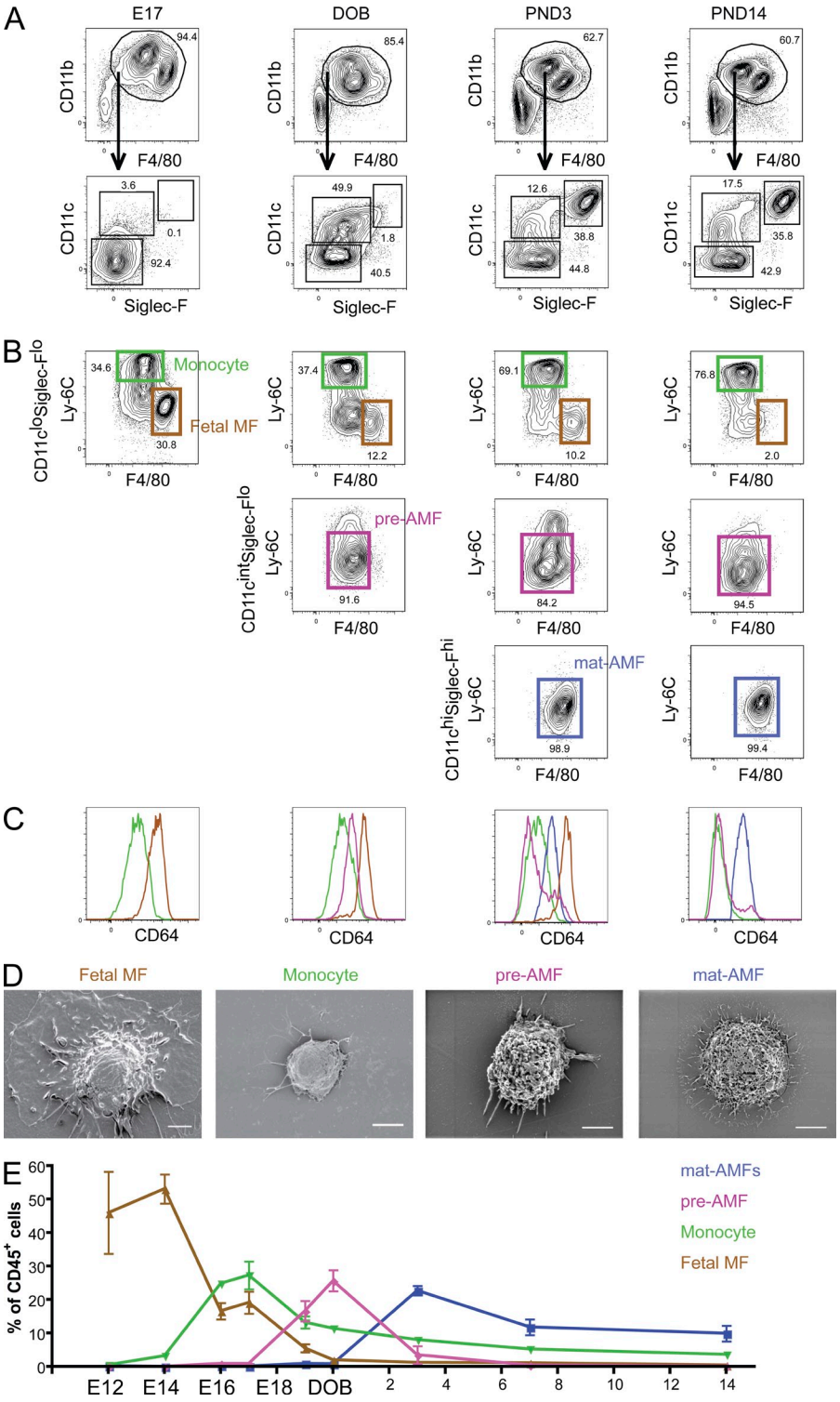


**Figure 3. Fetal MFs, fetal monocytes, preAMFs, and mature AMFs appear in consecutive waves during lung development.** Lungs were harvested at various time points before and after (PND3, PND14) the date of birth (DOB). CD11b$^{+}$F4/80$^{+}$ myeloid cells were subdivided into CD11c$^{lo}$Sigle-F$^{lo}$, CD11c$^{int}$Sigle-F$^{lo}$, and CD11c$^{hi}$SiglecF$^{hi}$ cells (A) and analyzed for Ly-6C, F4/80 (B), and CD64 expression (C). (D) Fetal monocytes (isolated at E17), fetal MFs (isolated at E17), preAMFs (isolated at the DOB), and mature AMFs (isolated from adult mice) were sorted, put in culture in vitro overnight in complete medium, and subjected to electromagnetic microscopy to assess their capacity to adhere to cell culture plastic and general morphology. (E) Percentage of fetal MFs, fetal monocytes, preAMFs, and mature AMFs among CD45$^{+}$ cells in the lungs at the indicated time points. Data in A–E represent at least two independent experiments involving at least three independent mice per time point.

cells among mature AMFs only dropped very slowly during adult life (Fig. 4 D), suggesting that transferred monocytes gave rise to a stable self-maintaining population.

### GM-CSF drives the development of preAMFs around birth

Primary pulmonary alveolar proteinosis (PAP) is a disease associated with the accumulation of surfactant in the lungs that has been linked to nonfunctional GM-CSF signaling in patients (Suzuki et al., 2008) and could be reproduced in genetically modified mice lacking GM-CSF (*Csf2*$^{-/-}$) or GM-CSF-R (*Csf2r*$^{-/-}$) expression (Huffman et al., 1996; Reed et al., 1999; Reed et al., 2000; Zsengellér et al., 1998). Although the PAP syndrome was originally proposed to derive from the fact that AMFs were not functional in these mice (REFs; Golde, 1976,

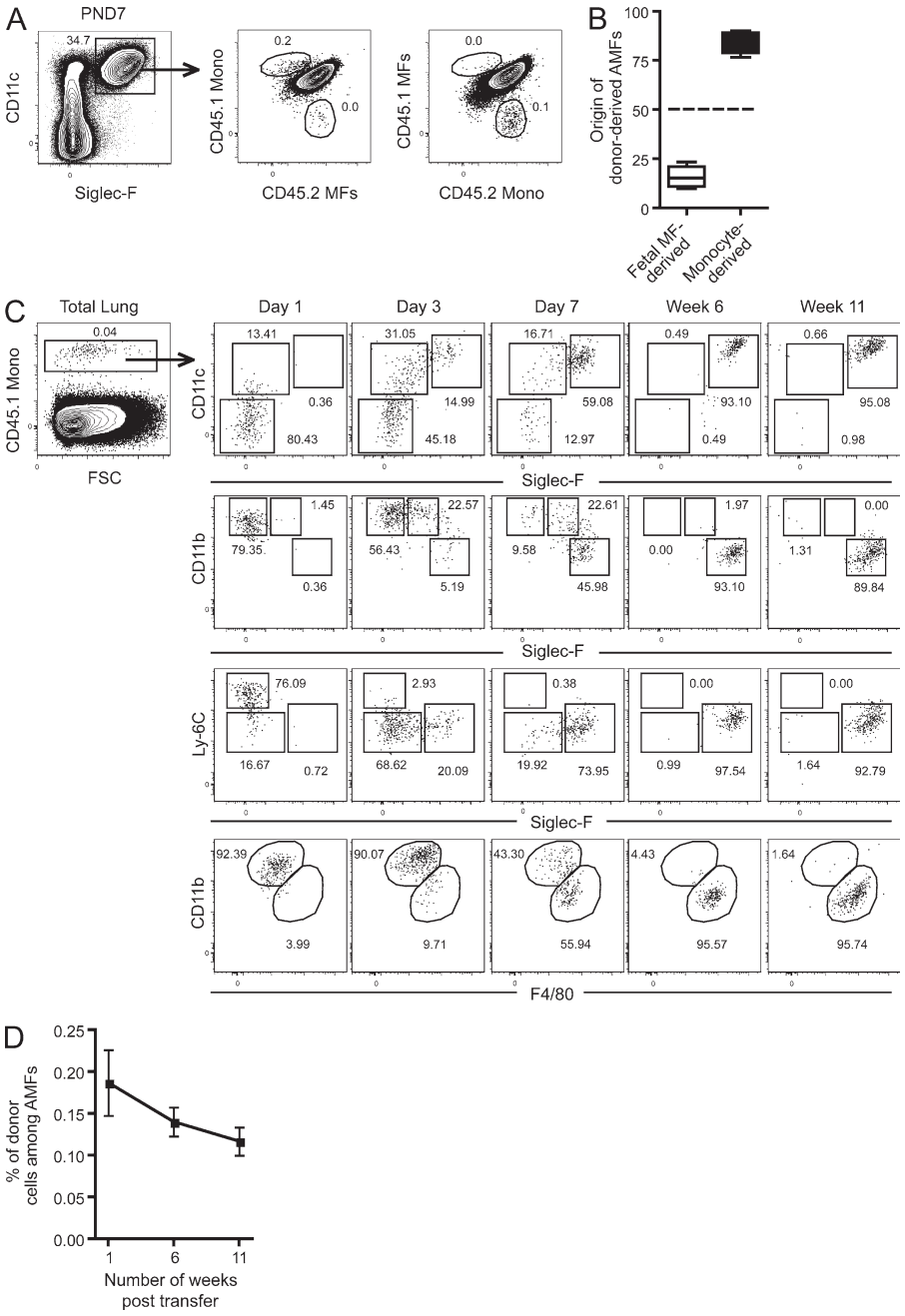


**Figure 4. Fetal monocytes give rise to self-maintaining AMFs through a preAMF intermediate step.** (A and B) CD45.1+ or CD45.2+ E17 embryos were sacrificed and fetal monocytes and fetal MFs were FACS sorted and mixed together at a 50:50 ratio (A; left, CD45.1+ fetal monocytes and CD45.2+ fetal MFs; right, CD45.1+ fetal MFs and CD45.2+ fetal monocytes) and transferred into CD45.1+CD45.2+ mice on their DOB. 7 d after transfer, CD45.1+CD45.2+ recipient mice were sacrificed and the presence of CD45.1+ or CD45.2+ donor-derived AMFs was evaluated. (B) Summary of data from four independent recipient mice. (C) CD45.1+ E17 embryos were sacrificed, and fetal monocytes were FACS sorted and transferred into CD45.2+ mice on their DOB. At the indicated time points after transfer, the expression of CD11c, CD11b, Ly-6C, SiglecF, and F4/80 was evaluated in CD45.1+ fetal monocyte–derived cells. (D) The percentage of CD45.1+ fetal monocyte–derived cells among mature AMFs at the indicated time points after transfer. Data represent at least two (A– D) independent experiments, with at least three recipient mice per time point.

1979; Harris, 1979; Gonzalez-Rothi and Harris, 1986; Nugent and Pesanti, 1983; LeVine et al., 1999; Yoshida et al., 2001; Paine et al., 2001; Thomassen et al., 2007), Shibata et al. (2001) later proposed that a MF developmental defect rather than a functional defect may lie at the basis of the disease. However, it is not known how absence of GM-CSF signaling impacts on AMF ontogeny before and shortly after birth. We found that lung epithelial cells show an increased expression of GM-CSF mRNA that is paralleled by high GM-CSF protein levels in lung tissues around DOB, yet quickly wanes thereafter (Fig. 5, A and B). Because fetal MFs, fetal monocytes, preAMFs, and mature AMFs all express the GM-CSF-R (CD116, Fig. 5 D), we decided to investigate the development of AMFs in *Csf2*$^{-/-}$ mice. On their DOB, *Csf2*$^{-/-}$ mice completely lacked preAMFs (Fig. 5 C). However, they contained fetal MFs and monocytes in ratios similar to WT mice (see Fig. 3 for comparison). Note that the small CD11c$^{int}$ population that was found in *Csf2*$^{-/-}$ mice on DOB was Ly-6C$^{int}$, but had a SiglecF$^{lo}$CD64$^{lo}$FSC$^{lo}$SSC$^{lo}$ profile. Therefore, the wave of preAMFs that is found in WT mice around birth is absent in *Csf2*$^{-/-}$ mice. Importantly, development of preAMFs or mature AMFs remained absent in *Csf2*$^{-/-}$mice throughout life (Fig. 5 E). Liver and splenic CD11b$^{int}$F4/80$^{hi}$-resident MFs, however, could be readily identified in *Csf2*$^{-/-}$ mice (Fig. 5, F and G). In contrast, we

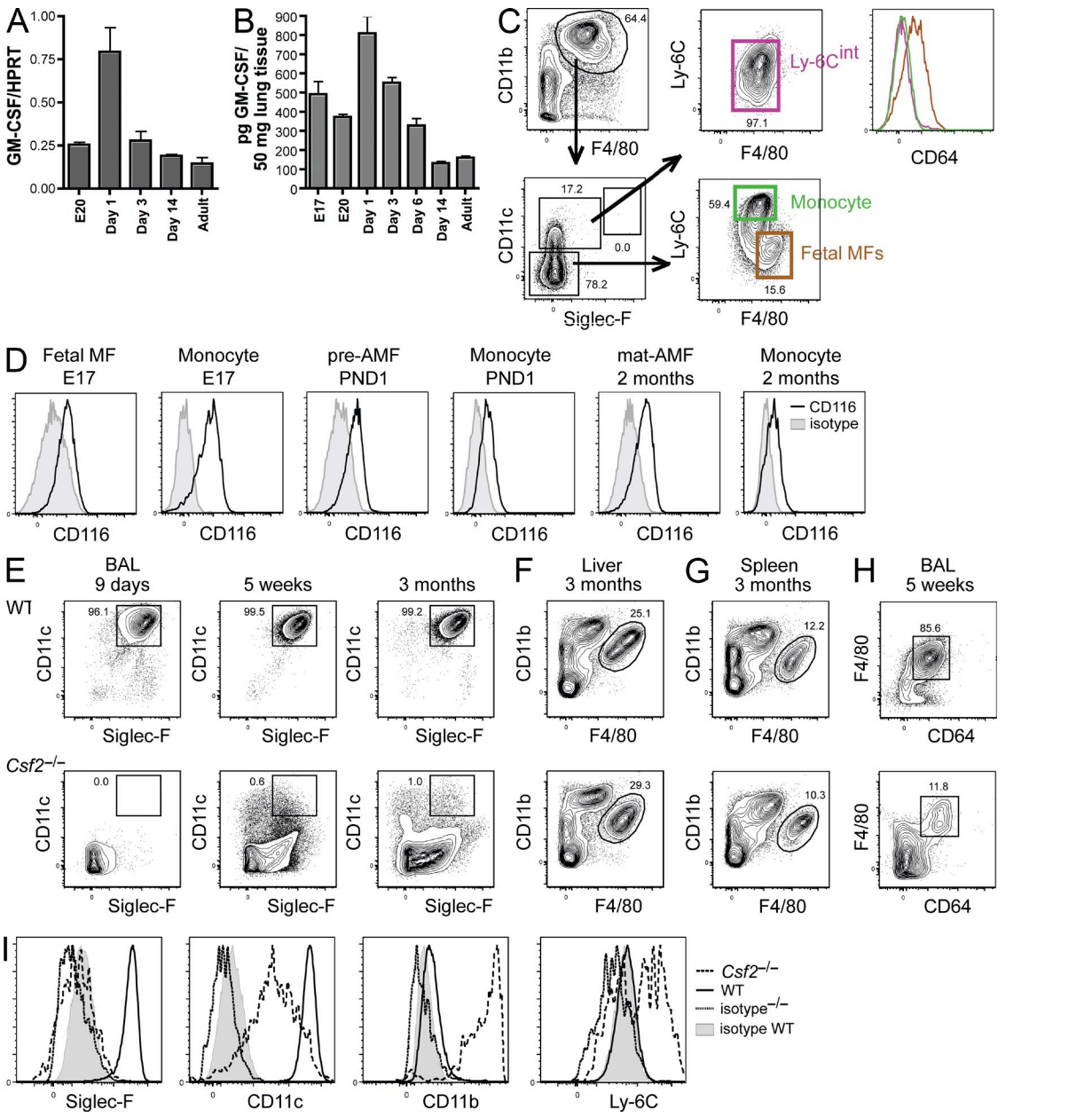


**Figure 5.** ***Csf2*$^{-/-}$ mice lack preAMFs and mature AMFs throughout life.** (A) Lung epithelial cells isolated at the indicated time points before and after birth were FACS sorted, and expression of GM-CSF mRNA was measured by RT-PCR. The expression levels were normalized by comparison with expression of the HPRT housekeeping gene. (B) GM-CSF levels in lung homogenates was measured by ELISA at the indicated time points before and after birth. (C) *Csf2*$^{-/-}$ mice were sacrificed on their DOB. Lungs were homogenized and CD11b$^{+}$F4/80$^{+}$ myeloid cells (gated as indicated) were assessed for Ly-6C, CD64, CD11c, F4/80, and SiglecF expression. (D) GM-CSF-R (CD116) expression was evaluated on fetal MFs, fetal monocytes, preAMFs, and mature AMFs on the days mentioned using the gating strategy depicted in Fig. 3. (E) The presence of CD11c$^{+}$SiglecF$^{+}$ AMFs was evaluated in the BAL of WT and *Csf2*$^{-/-}$ mice at the indicated time points after birth. (F and G) The presence of F4/80$^{hi}$CD11b$^{lo}$ splenic MFs and liver MFs (Kupffer Cells) was evaluated in adult WT and *Csf2*$^{-/-}$ mice. (H and I) BAL cells from adult WT and *Csf2*$^{-/-}$ mice were subjected to a Percoll gradient to remove dead cells and protein debris. The resulting CD64$^{+}$F4/80$^{+}$ MFs were assessed for Ly-6C, CD11b, CD11c, and SiglecF expression (I). Data represent two (H and I) and three (A–G) independent experiments.

had great difficulty identifying MFs in the BAL of *Csf2*$^{-/-}$ mice. Proteinosis had already developed by ∼4 wk of age and yielded autofluorescent debris in the BAL fluid. The presence of many dead cells (unpublished data) also rendered the analysis of the cellular composition of the BAL difficult. However, others have described AMFs with functional defects in adult *Csf2*$^{-/-}$ mice. To characterize these cells, we first performed a Percoll gradient to remove debris and dead cells form the BAL fluid and then used a more general MF gating strategy using F4/80 and CD64 (Fig. 5 H). In doing so, we could indeed

identify some rare F4/80$^{+}$CD64$^{+}$ cells in the BAL of *Csf2*$^{-/-}$ mice. These cells did not express a bona fide AMF profile, but were found to be SiglecF$^{lo}$CD11b$^{hi}$CD11c$^{int}$Ly-6C$^{hi\text{-}to\text{-}int}$. Moreover we could only identify such cells after 4 wk of age, i.e., once the first signs of PAP developed.

### Perinatal GM-CSF cytokine therapy restores the generation of self-maintaining preAMFs in *Csf2*$^{-/-}$ mice

Given the surge of GM-CSF expression in the perinatal period, and given the fact that AMFs can self-maintain throughout life once generated, we reasoned that perinatal recombinant GM-CSF treatment of *Csf2*$^{-/-}$ mice during the first days of life might be sufficient to rescue arrested AMF development. Treatment of neonatal *Csf2*$^{-/-}$ mice through local i.n. administration of rGM-CSF on 1, 3, or 5 consecutive days, lead to the dose-dependent development of cells with a CD11c$^{int}$SiglecF$^{int\text{-}hi}$ that resembled AMFs, but had lower expression of SiglecF, and had not yet down-regulated CD11b and up-regulated F4/80 as bona fide mature AMFs (Fig. 6, B and C). Such rescued *Csf2*$^{-/-}$ AMFs could self-maintain for several weeks after the rGM-CSF treatment (Fig. 6 C), but were unable to significantly inhibit the development of PAP, as measured by the amount of protein content in the BAL fluid, suggesting that they were not only phenotypically but also functionally immature (Fig. 6 D). To verify whether these rGM-CSF–rescued immature AMFs were irreversibly blocked in the immature AMF stage or whether these cells merely lacked the proper cellular environment to differentiate into mature AMFs we designed a transfer experiment in which immature CD11c$^{hi}$SiglecF$^{int}$CD11b$^{hi}$ AMFs from cytokine-treated CD45.2 *Csf2*$^{-/-}$ mice were transferred into a neonatal WT CD45.1 GM-CSF replete hosts (Fig. 7). The phenotype of transferred cells was evaluated 2, 9, and 42 d after transfer. As shown in Fig. 7, immature AMFs gradually further increased expression of CD11c, SiglecF, F4/80, and CD64 expression and, as a final step in their maturation process, down-regulated CD11b expression until they were undistinguishable from mature AMFs.

## DISCUSSION

It is a long-held belief that all MFs develop from circulating monocytes and constitute a unified MPS, but MFs have

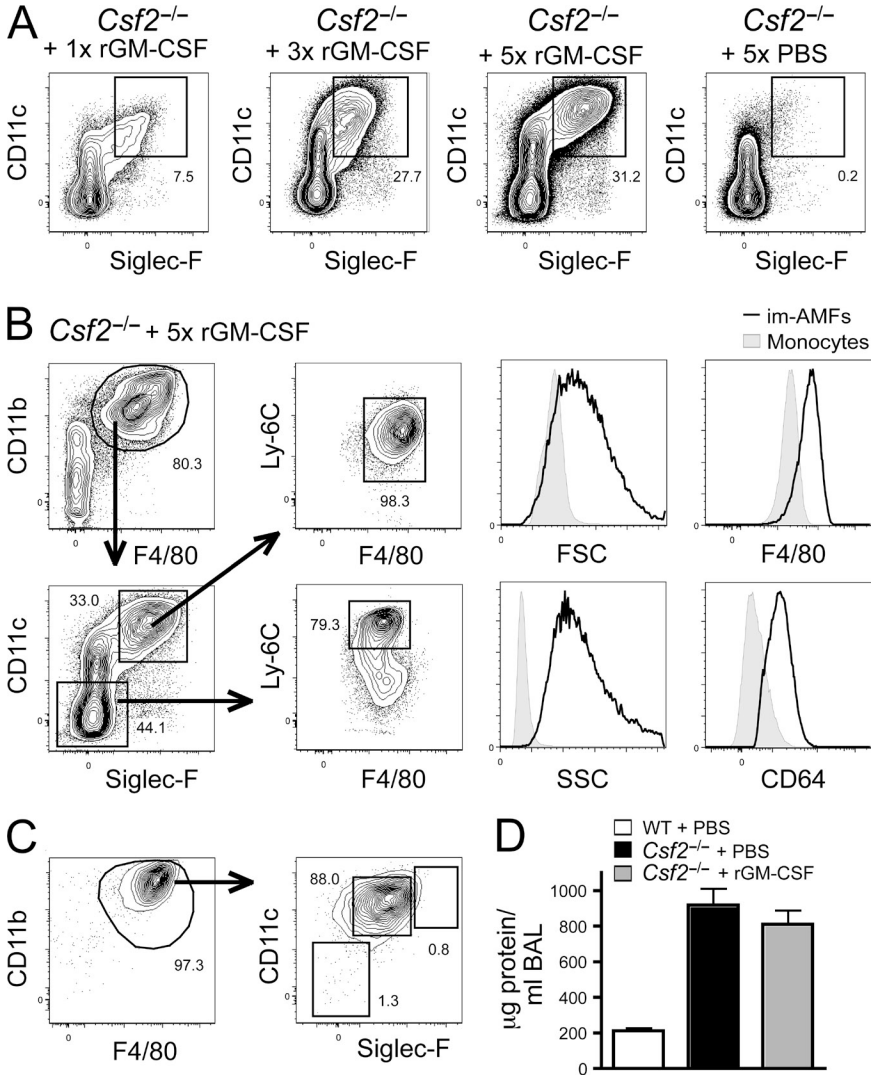


**Figure 6. Perinatal GM-CSF treatment of *Csf2*$^{-/-}$ mice restores the generation of self-maintaining preAMFs.** (A and B) *Csf2*$^{-/-}$ mice were treated 1 time (1x) on the first day after birth, 3 times (3x) on the first 3 d after birth, or 5 times (5x) on the first 5 d of birth with rGM-CSF or PBS i.n. (1 rGM-CSF or PBS treatment per day). rGM-CSF–treated or PBS-treated *Csf2*$^{-/-}$ mice were sacrificed on PND 7. (A) Lungs were homogenized and CD11b$^{+}$F4/80$^{+}$ myeloid cells were assessed for CD11c and SiglecF expression. (B) Expression of FSC, SSC, Ly-6C, CD64, CD11c, F4/80, and SiglecF on SiglecF$^{lo}$CD11c$^{lo}$CD11b$^{hi}$Ly-6C$^{hi}$ monocytes and SiglecF$^{int}$CD11c$^{hi}$CD11b$^{hi}$Ly-6C$^{hi}$ immature AMFs harvested from *Csf2*$^{-/-}$ mice treated for 5 consecutive days with rGM-CSF. (C) 5 wk after 5 consecutive rGM-CSF treatments, *Csf2*$^{-/-}$ mice were sacrificed and the presence of CD11c$^{+}$SiglecF$^{+}$ cells in the BAL was evaluated. (D) WT or *Csf2*$^{-/-}$ mice treated with 5 consecutive treatments of rGM-CSF or PBS were sacrificed at 7 wk of age, and the development of alveolar proteinosis was evaluated by measuring the protein concentration in the BAL. Data represent two (D) and three (A– C) independent experiments, with at least three recipient mice per time point.

recently been shown to develop from primitive precursors before birth (Geissmann et al., 2010). Both pathways of development might be mutually exclusive or coexist. Indeed, microglia originate directly from yolk sac MFs that colonize the brain before birth, and then self-maintain throughout life without any input from BM-derived precursors (Ajami et al., 2007; Ginhoux et al., 2010). However, we and others have shown that intestinal MFs derive directly from BM-derived monocytes that continuously seed the lamina propria and differentiate locally into MFs (Bogunovic et al., 2009; Varol et al., 2009; Tamoutounour et al., 2012). The specific cellular origin of other tissue-resident MFs remains unknown, but elegant fate-mapping experiments have demonstrated that BM-derived precursors contribute minimally to the pool of most tissue-resident MFs across tissues (Schulz et al., 2012; Yona et al., 2013). Based on analogy with microglia, it was proposed therefore that most tissue-resident MFs may follow the microglia model and originate from yolk sac MFs (Gomez Perdiguero et al., 2013).

Here, using radiation chimeric mice, parabiosis, and adoptive cellular transfer models, we investigated the ontogeny of AMFs. Confirming the $CX_3CR1$-monocyte fate-mapping studies in adult mice (Yona et al., 2013), we demonstrate that circulating BM-derived monocytes contribute only minimally to the pool of AMFs, except when mice are lethally irradiated, emptying the AMF niche. We therefore conclude that there must be a self-maintaining, proliferating pool of MFs in the lung. During the completion of this manuscript, another group reported similar conclusions, showing that this pool of self-maintaining lung MFs can even fill up the AMF niche after AMF depletion caused by influenza infection or DT-mediated depletion (Hashimoto et al., 2013).

The fact that adult circulating monocytes only minimally feed the steady-state AMF pool suggested an embryonic

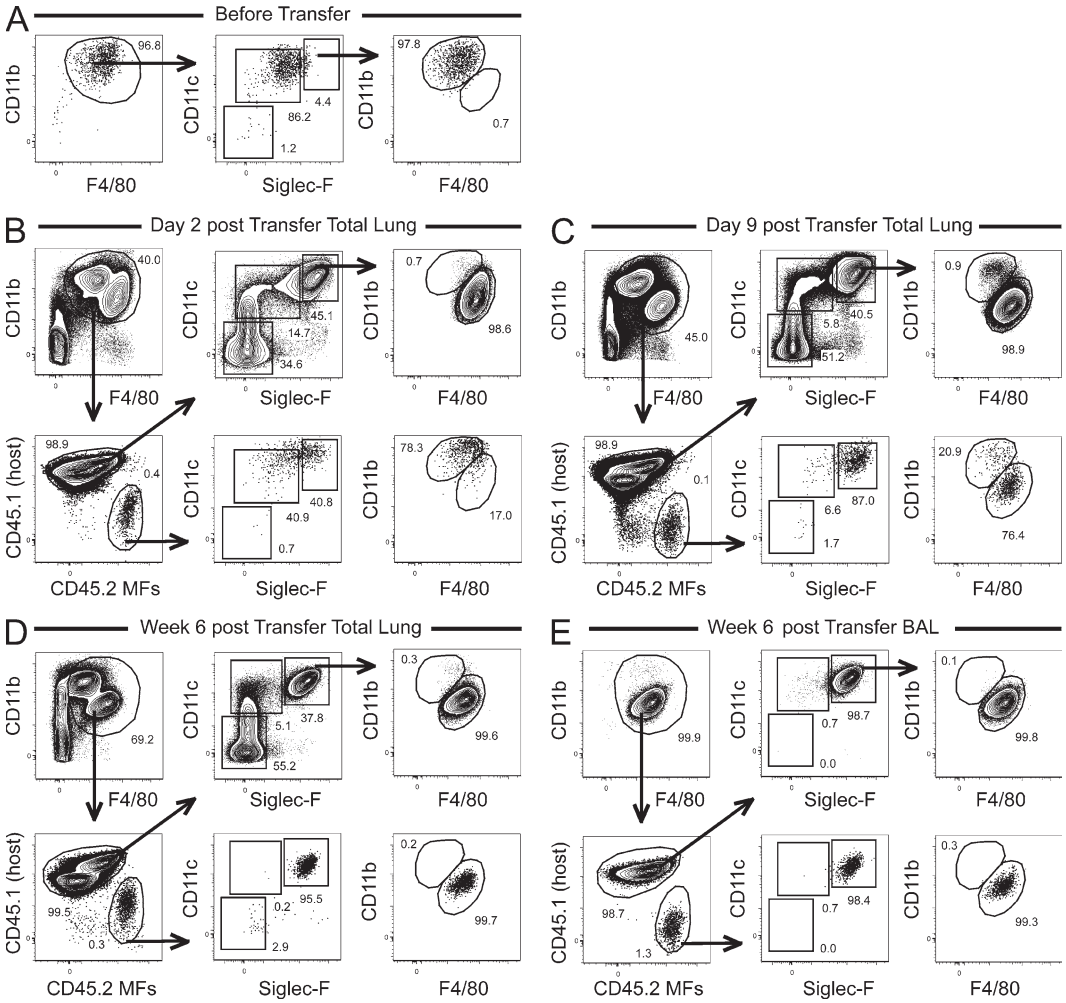


**Figure 7. Terminal differentiation of GM-CSF–rescued immature AMFs requires a GM-CSF–replete host.** *Csf2*$^{-/-}$ mice treated with 5 consecutive treatments of rGM-CSF were sacrificed at 7 d of age. The lungs were homogenized and CD45.2$^+$ CD11c$^{int}$SiglecF$^{int}$ preAMFs were FACS sorted (profile of the sorted cells before transfer is shown in A) and transferred into CD45.1$^+$ WT mice on their DOB. 2 d, 9 d, and 6 wk after transfer, CD45.1$^+$ recipient mice were sacrificed, and the presence of CD45.2$^+$ donor-derived cells was evaluated in the lungs (B–D) and BAL (E). Their CD11b, F4/80, CD11c, and SiglecF expression profile was also assessed. Data represent two independent experiments with at least three recipient mice per time point.

precursor, and decided to take a closer look at the nature of this embryonic precursor. In our developmental analysis, we did not solely rely on expression of the pan MF markers CD64, F4/80, and CD11b, but also took advantage of the unique and discriminating surface characteristics of mature AMFs that express high levels of SiglecF and CD11c. A clearly defined phenotype of the mature tissue-resident MF, allowed us to also look for intermediate steps in AMF development, a task almost impossible for other tissue-resident MFs for which such late maturation markers are often lacking. The early developing lung (E12, before fetal liver hematopoiesis has started) contained mainly F4/80$^{hi}$ CD11b$^{int}$ Ly-6C$^{-}$ CD64$^{hi}$ cells that had a phenotype and ultrastructure like primitive MFs and did not express AMF markers. From E14 onwards, we also observed a steady increase in fetal monocytes in the developing lung. As definitive hematopoiesis starts only from E16.5, these were most likely derived from fetal liver hematopoiesis (Costa et al., 2012). Cells with a preAMF phenotype started accumulating in the fetal lung around the saccular stage of lung development (E18.5), when branching canaliculi become narrower and give rise to saccules, which are the precursors to alveoli (Morrisey and Hogan, 2010). Bona fide mature SiglecF$^{hi}$CD11c$^{hi}$ AMFs only appeared during the first week after birth, and not before birth, as shown for microglia (Ginhoux et al., 2010).

As both fetal monocytes and fetal MFs were found in the developing lung, the question remained as to which of these two were the progenitor to AMFs. Based on kinetic analysis, phenotypic changes after adoptive transfer, and competitive reconstitution experiments, we concluded that fetal monocytes were the main progenitors to AMFs. First, adoptive transfer of E17 fetal monocytes was much more efficient in generating long-term engraftment of AMFs compared with transfer of E17 fetal MFs. Second, when E17 fetal monocytes were transferred and followed over time, they differentiated gradually into AMFs, first down-regulating Ly-6C and acquiring CD11c expression, followed by SiglecF acquisition. The final step of AMF maturation was accompanied by further up-regulation of SiglecF, down-regulation of CD11b and up-regulation of F4/80. This entire process took ∼7 d, which would also fit with the kinetics of appearance of the first lung fetal monocytes (E14) over an intermediate stage preAMF stage around DOB and with the appearance of mature AMFs at PND1-3. Third, when adoptively transferred, fetal monocytes gave rise to a long-term population of AMFs that were almost not diluted over time. Others have shown, using fate mapping experiments, that AMFs do not derive from E7 Runx1$^{MER\text{-}Cre\text{-}MER}$ *Rosa*-LSL-YFP–tagged yolk sac MFs (Ginhoux et al., 2010) or from adult CX3CR1$^{ER.Cre}$ *Rosa*-LSL-YFP–tagged mononuclear cells (Yona et al., 2013), but have offered no explanations as to where exactly AMFs do derive from. Our study provides direct evidence that fetal monocytes are the predominant progenitor to AMFs. One group has proposed, using an inducible *Mx*Cre-driven Myb deficiency abolishing adult hematopoietic cells, a mixed origin of lung MFs, partly deriving from adult hematopoietic and partly from Myb-independent primitive precursors, although it was hard to conclude from the gating strategy whether AMFs were included in the analysis, and whether other myeloid populations expressing F4/80 such as eosinophils were excluded from analysis (Schulz et al., 2012). This group also showed that in Myb-deficient embryos, which lack fetal monocyte development, an F4/80$^{hi}$ MF population was present in the fetal lung. However, as these Myb-deficient embryos never reach term and die from severe anemia at E16.5, it is not possible to assess whether these F4/80$^{hi}$ MFs would indeed become AMFs, as AMFs only appear after birth. Moreover, the F4/80$^{hi}$ cells identified in the lungs of the *Myb*-deficient embryos around E16 are most likely the primitive yolk sac MFs that we also see peaking around this time point in WT mice (Fig. 3).

It is remarkable that fetal MFs and monocytes were described by Ginhoux et al. (2010) to colonize the developing skin at the same time points as we recovered them in the developing lung, with fetal monocytes giving rise to a specialized subset of dendritic cells called LCs (Hoeffel et al., 2012). In fact, AMFs and LCs share several unique features: (a) they populate a cellular niche where they constitute the only antigen-presenting cell in the steady state (the alveoli and the epidermis, respectively); (b) the alveolar and the epidermal niche are not easily accessible to hematopoietic precursors as these are barriers to the outside world, probably requiring the LCs and AMFs to self-maintain in the steady state; (c) AMFs (this study) and LCs (Chorro et al., 2009; Hoeffel et al., 2012) colonize their niches in a single wave during the first week after birth; and (d) fate-mapping studies demonstrate that AMFs (Ginhoux et al., 2010) and LCs (Hoeffel et al., 2012) do not derive from yolk sac MFs, but instead derive primarily from fetal monocytes (this study; Hoeffel et al., 2012).

The environmental cues that drive AMF and LC differentiation, however, seem to differ significantly. LCs require IL-34, but not M-CSF or GM-CSF (Greter et al., 2012a; Greter et al., 2012b; Wang et al., 2012), whereas AMFs require GM-CSF and M-CSF, but not IL-34 for their development (this study; Wang et al., 2012; Hashimoto et al., 2013). Around the perinatal period, we noticed high expression of GM-CSF mRNA in epithelial cells and protein in BAL fluid, but this waned rapidly after birth. Analysis of *Csf2*$^{-/-}$ mice demonstrated that lungs were completely devoid of AMFs, identifying GM-CSF as the driving cytokine for AMF development in the perinatal period. Previous work on *Csf2*$^{-/-}$ or *Csf2r*$^{-/-}$ mice with pulmonary alveolar proteinosis (PAP) reached conflicting results stating that AMF function was impaired (Golde, 1976, 1979; Harris, 1979; Nugent and Pesanti, 1983; Gonzalez-Rothi and Harris, 1986; LeVine et al., 1999; Yoshida et al., 2001; Paine et al., 2001; Thomassen et al., 2007), or that AMF development was abnormal (Shibata et al., 2001). Here, we show that AMF development is blocked before the preAMF stage, and the few MFs that are found in *Csf2*$^{-/-}$ mice are most likely inflammatory MFs that accumulate in response to lung damage inflicted by surfactant accumulation. Given the boost of GM-CSF expression in the perinatal period, and

given the fact that AMFs can self-maintain throughout life once generated, we reasoned that perinatal recombinant GM-CSF treatment of *Csf2*$^{-/-}$ mice during the first days of life might be sufficient to rescue arrested AMF development. Perinatal GM-CSF for 5-d treatment, indeed, rescued long-term CD11c$^{hi}$SiglecF$^{int}$ AMF development, AMFs appeared in the alveolar lumen, but these AMFs were in an immature state, failing to down-regulate CD11b and to prevent PAP. It is possible that 5 d of GM-CSF treatment of *Csf2*$^{-/-}$ mice was insufficient to cause full AMF differentiation, or that continuous low-level GM-CSF production in a replete host induces a second signal permissive to terminal AMF differentiation. In support, adoptive transfer of immature AMFs from GM-CSF–treated *Csf2*$^{-/-}$ mice to WT mice allowed the terminal differentiation of immature AMFs, a process that took a few days. We can only speculate as to what exactly this second signal might be. Previous work identified PPARγ as a crucial transcription factor for AMF development necessary to prevent PAP (Baker et al., 2010; Gautier et al., 2012a). GM-CSF induces PPARγ gene expression (Bonfield et al., 2003). However, we administered the PPARγ agonist rosiglitazone in the perinatal period, and this failed to terminally differentiate AMFs in GM-treated *Csf2*$^{-/-}$ mice (unpublished observations). Studies in humanized mice confirm the essential role of GM-CSF in human AMF development. Mouse GM-CSF does not bind to human GM-CSF-R, and therefore these humanized mice do not possess human AMFs. Mice in which the mouse *Csf2* locus was replaced by the human coding sequence lacked murine AMFs (Willinger et al., 2011), and without engraftment of human HSCs they developed PAP. After human HSC engraftment, MFs of human origin were found in the BAL, but these MFs were incapable of fully protecting against PAP. This suggests that, in humans as well as in mice, GM-CSF alone may not be sufficient to generate fully functional and terminally differentiated AMFs. Strikingly, a recent paper also identified GM-CSF as the cytokine necessary for the proliferation and self-maintenance of AMFs after local depletion from the lungs (Hashimoto et al., 2013).

In conclusion, we have elucidated the pathway of AMF development by showing that fetal monocytes develop into preAMFs around the time that airspaces (fluid filled sacculi) start to occur during lung development. At the DOB, most preAMFs are still in the alveolar septa, but shortly thereafter they end up in the alveolar space as immature AMFs, and then rapidly down-regulate CD11b and become functionally mature cells that self-maintain and do not require input from circulating hematopoietic precursors. Importantly, the appearance of such preAMFs seems to be restricted to a single wave around birth and accompanied by a boost of GM-CSF around this period, which is necessary for proper AMF instruction. In the broader context of MF development, we provide evidence for a third model for the origin of tissue-resident MF, whereby AMFs originate from fetal monocytes during the perinatal period. It remains to be investigated whether other tissue-resident MFs follow the microglia model (yolk sac MF origin), the intestinal MF model (BM-monocyte origin), or the AMF/LC model (fetal-monocyte origin).

## MATERIALS AND METHODS

**Mice.** C57BL/6 CD45.2$^{+}$, congenic C57BL/6 CD45.1$^{+}$ (The Jackson Laboratory), *Csf2*$^{-/-}$ and *Ccr2*$^{-/-}$ mice were bred at the animal facility of the University of Ghent. For timed pregnancies, female C57B1/6 or GM-CSF mice were superovulated with 2 i.u. pregnant mare serum gonadotropin (Folligon; Intervet) to stimulate follicle growth and 2 i.u. human chorionic gonadotropin (Chorulon; Intervet) to induce ovulation. Mice were housed under specific pathogen–free conditions in individually ventilated cages in a controlled day–night cycle and given food and water ad libitum. All experiments were approved by the animal ethical committee of the University of Ghent.

**Generation of BM chimeras and parabiotic mice.** C57BL/6 (CD45.1$^{+}$ CD45.2$^{+}$) mice were lethally irradiated with two doses of 5.5 Gy, and received i.v. 2 × 10$^{6}$ BM cells consisting of a 50:50 mix of BM cells obtained from femurs and tibias of WT C57BL/6 CD45.1$^{+}$ and of C57BL/6 *Ccr2*$^{-/-}$ CD45.2$^{+}$ mice. 7 wk after reconstitution, proper blood chimerism was verified, and mice were analyzed 8 wk after BM transfer.

Parabiotic mice were generated by suturing weight-matched CD45.1$^{+}$ and CD45.2$^{+}$ mice of 9 wk of age. Parabiotic mice were then kept under Bactrim for 2 mo before analysis. As previously described (Liu et al., 2007), circulating B cells and T cells equilibrated to almost 50% chimerism at that time, indicating efficient exchange between the joined mice.

**BrdU labeling in vivo and cell cycle analysis.** Mice were injected i.p. with 1.5 mg BrdU (Sigma-Aldrich) to ensure its immediate availability, and their drinking water was supplemented for up to 28 d with 0.8 mg/ml of BrdU and 2% glucose and changed daily. Lung cells were stained first for surface markers and then permeabilized for BrdU staining (BrdU labeling Flow kit; BD). Ki-67 staining (BD) was performed using the staining protocol corresponding to the Foxp3 labeling Flow kit (eBioscience).

**Flow cytometry and cell sorting.** Flow cytometric studies were performed using a LSRII (BD) with subsequent data analysis using FlowJo software (Tree Star). Cell sorting was performed on a FACSAria II cytometer. After cell sorting, purity was checked (always >95%). For flow cytometry, lungs were cut into small pieces, incubated in RPMI containing Liberase TM (Roche) and DNase (Roche), and then syringed through a 19-gauge needle to obtain a homogenous cell suspension. Red blood cells were lysed for 4 min at room temperature in 1 ml osmotic lysis buffer. For flow cytometry of BAL derived from GM-CSF mice diagnosed with proteinosis, BAL cells were first enriched using a Percoll gradient (Sigma-Aldrich).

Fluorochrome- or biotin-conjugated mAbs specific for mouse CD11c (clone N418), CD3 (clone 145-2C11), CD19 (clone 1D3), Ly-6G (clone 1A8), CD11b (clone M1/70), CD64 (clone X54-5/7.1), Ly-6C (clone AL21), SiglecF (clone E50-2440), SAV, Ki-67 (clone B56), Sca-1 (clone d7), CD45.1 (clone A20), and CD45.2 (clone 104); the corresponding isotypes; and the secondary reagent PE-Texas red–conjugated streptavidin were all purchased from BD or eBioscience. Anti-MHCII (clone M5/114) and anti-Epcam (clone G8.8) were purchased from BioLegend. Anti-F4/80 (clone A3-1) was purchased from Serotec. Neutrophils (Ly-6G$^{hi}$CD11b$^{hi}$CD64$^{lo}$ Ly-6C$^{hi}$ cells), Eosinophils (SiglecF$^{hi}$CD11b$^{hi}$CD64$^{lo}$Ly-6C$^{int}$ cells), T cells (CD3$^{hi}$CD11b$^{lo}$CD64$^{lo}$ cells), and B cells (CD19$^{hi}$CD11b$^{lo}$CD64$^{lo}$ cells) were systematically outgated before analysis. Fixable live/dead marker Aqua was purchased from Invitrogen. Dead cells were outgated using the live/marker before analysis.

**Transfer of sorted cells.** Fetal monocytes and fetal MFs were sorted from the lungs of time-mated E17 C57BL/6 CD45.2$^{+}$ and CD45.1$^{+}$ embryos.

After sorting, fetal monocytes and fetal MFs from different donors were mixed in a 1:1 ratio and administered i.n. into the lungs of day 1 C57BL/6 CD45.1$^+$ x CD45.2$^+$ recipients under Isoflurane anesthesia ($4 \times 10^4$ cells in 7 µl PBS per neonate). Lungs were obtained and analyzed during a follow-up period of 11 wk total. In another experiment, preAMF were sorted from the lungs of neonatal *Csf2*$^{-/-}$ mice treated for 5 consecutive days with rGM-CSF i.n. Sorted preAMF cells were administrated i.n. into the lungs of day 1 WT mice ($4 \times 10^4$ cells in 7 µl PBS per neonate). Lungs were obtained and analyzed 2 and 9 d after transfer.

**RT-PCR and GM-CSF ELISA.** For RT-PCR–sorted cells were frozen and cell pellets were homogenized in Tripure Reagent (Roche). RNA was isolated according to the manufacturer's protocol. 500 ng RNA was reverse transcribed using the Transcriptor High Fidelity cDNA Synthesis kit (Roche) with random hexamers. The obtained cDNA was used for real time quantitative PCR. SYBR Green Master (Roche) was used, and the expression levels were normalized by comparison with hypoxanthine-guanine phosphoribosyl transferase (HPRT) expression. All reactions were performed in a LCII 480 (Roche).

To measure GM-CSF levels in naive lungs, ELISA was performed on lung homogenates. Naive lungs were snap frozen in liquid nitrogen and stored at −80°C. The lungs were then homogenized with a tissue homogenizer in 500 µl of cold lysis buffer (20 mM Tris-HCl, pH 8.0, 0.14 M NaCl, 10% glycerol [vol/vol], 1 mM PMSF, 1 mM sodium orthovanadate [Na3VO4], 1 µM NaF, 40 mg/ml aprotinin, and 20 mg/ml leupeptin) using a tissue homogenizer (IKA) with the addition of 1% Igepal after homogenization. Samples where then kept on ice for 30 min, with agitation every 10 min, followed by a centrifugation to pellet debris. Supernatants were frozen at −80°C. GM-CSF levels in these supernatants were measured by ELISA (eBioscience) according to the manufacturer's protocol. Concentrations were corrected for the weight of the lungs.

**Immunohistochemistry.** Lungs were inflated with PBS/OCT (1:1) and fixed in 4% paraformaldehyde/PBS, pH 7.4, for 24 h. Tissue was then washed in 70% ethanol, dehydrated in series of alcohols, and embedded in paraffin, followed by processing for H&E staining. Separate lung cryosections of 4 µm were also made on frozen lungs, and then stained with DAPI and immunostained with Anti-SiglecF (CD170; Antibodies Online GmbH), secondary antibody staining and processing for confocal analysis (LSM710; Carl Zeiss).

**Electron microscopy.** Cells were seeded in 24-well plates (Nunc; CellSeed Inc. Labware). The next day, the cells were washed with PBS and fixed in 0.15 M cacodylate buffer with 2.5% paraformaldehyde and 2% glutaraldehyde for 2 h. After five 3-min washes with 0.15 M cacodylate buffer, the cells were treated with 2% osmium in 0.15 M cacodylate buffer for 30 min. Five 3-min washes with ultrapure water were followed by 5-min incubations in increasing concentrations of EtOH (25, 30, 50, 75, 90, 95, and 100%) and two 5-min incubations in 3-hydroxy-4,5-dimethyl-2(5H)-furanone (HDMF). After removal of HDMF, the cells were dried overnight. The plastic wells with the cells were mounted on a stub and coated with 5 nm of platinum in a Quorum sputter coater. The samples were imaged in an Auriga SEM (Carl Zeiss) at 1.5 kV, making use of an InLens secondary electron detector.

**Statistics.** Comparative experiments were tested for statistical significance using the unpaired Student's *t* test using Prism software (version 4.0; GraphPad). Differences were considered significant when $P < 0.05$.

We sincerely thank Saskia Lippens and Anneke Kremer of the VIB Bio-Imaging Core Facility for most valuable help with scanning EM pictures.

This work was supported by a European Research Council consolidator grant to B.N. Lambrecht, by a University of Ghent Multidisciplinary Research Partnerships grant (GROUP-ID consortium) to B.N. Lambrecht, by a Marie Curie re-integration grant (CIG), a Belspo Return Grant, a Post-Doc FWO grant and a Odysseus Grant to M. Guilliams, and by a FWO project grant to H. Hammad. I. De Kleer is the recipient of a European Respiratory Society/Marie Curie Joint Research Fellowship number MC 1231-2009 and of a Marie Curie Inter-European Fellowship (FP7-PEOPLE-2009-IEF, grant agreement number 253370). This work was also supported by Centre National de la Recherche Scientifique, Institut National de la Santé et de la Recherche Médicale, and European Communities (MUGEN Network of Excellence and MASTERSWITCH Integrating Project) for B. Malissen and S. Henri.

The authors have no conflicting financial interests.

**Submitted: 7 June 2013**
**Accepted: 3 September 2013**

## REFERENCES

Ajami, B., J.L. Bennett, C. Krieger, W. Tetzlaff, and F.M. Rossi. 2007. Local self-renewal can sustain CNS microglia maintenance and function throughout adult life. *Nat. Neurosci.* 10:1538–1543. http://dx.doi.org/10.1038/nn2014

Ajami, B., J.L. Bennett, C. Krieger, K.M. McNagny, and F.M. Rossi. 2011. Infiltrating monocytes trigger EAE progression, but do not contribute to the resident microglia pool. *Nat. Neurosci.* 14:1142–1149. http://dx.doi.org/10.1038/nn.2887

Bain, C.C., C.L. Scott, H. Uronen-Hansson, S. Gudjonsson, O. Jansson, O. Grip, M. Guilliams, B. Malissen, W.W. Agace, and A.M. Mowat. 2013. Resident and pro-inflammatory macrophages in the colon represent alternative context-dependent fates of the same Ly6Chi monocyte precursors. *Mucosal Immunol.* 6:498–510. http://dx.doi.org/10.1038/mi.2012.89

Baker, A.D., A. Malur, B.P. Barna, S. Ghosh, M.S. Kavuru, A.G. Malur, and M.J. Thomassen. 2010. Targeted PPARgamma deficiency in alveolar macrophages disrupts surfactant catabolism. *J. Lipid Res.* 51:1325–1331. http://dx.doi.org/10.1194/jlr.M001651

Bogunovic, M., F. Ginhoux, J. Helft, L. Shang, D. Hashimoto, M. Greter, K. Liu, C. Jakubzick, M.A. Ingersoll, M. Leboeuf, et al. 2009. Origin of the lamina propria dendritic cell network. *Immunity.* 31:513–525. http://dx.doi.org/10.1016/j.immuni.2009.08.010

Bonfield, T.L., C.F. Farver, B.P. Barna, A. Malur, S. Abraham, B. Raychaudhuri, M.S. Kavuru, and M.J. Thomassen. 2003. Peroxisome proliferator-activated receptor-gamma is deficient in alveolar macrophages from patients with alveolar proteinosis. *Am. J. Respir. Cell Mol. Biol.* 29:677–682. http://dx.doi.org/10.1165/rcmb.2003-0148OC

Bouwens, L., M. Baekeland, R. De Zanger, and E. Wisse. 1986a. Quantitation, tissue distribution and proliferation kinetics of Kupffer cells in normal rat liver. *Hepatology.* 6:718–722. http://dx.doi.org/10.1002/hep.1840060430

Bouwens, L., D.L. Knook, and E. Wisse. 1986b. Local proliferation and extrahepatic recruitment of liver macrophages (Kupffer cells) in partial-body irradiated rats. *J. Leukoc. Biol.* 39:687–697.

Chorro, L., A. Sarde, M. Li, K.J. Woollard, P. Chambon, B. Malissen, A. Kissenpfennig, J.B. Barbaroux, R. Groves, and F. Geissmann. 2009. Langerhans cell (LC) proliferation mediates neonatal development, homeostasis, and inflammation-associated expansion of the epidermal LC network. *J. Exp. Med.* 206:3089–3100. http://dx.doi.org/10.1084/jem.20091586

Costa, G., V. Kouskoff, and G. Lacaud. 2012. Origin of blood cells and HSC production in the embryo. *Trends Immunol.* 33:215–223. http://dx.doi.org/10.1016/j.it.2012.01.012

Gautier, E.L., A. Chow, R. Spanbroek, G. Marcelin, M. Greter, C. Jakubzick, M. Bogunovic, M. Leboeuf, N. van Rooijen, A.J. Habenicht, et al. 2012a. Systemic analysis of PPARγ in mouse macrophage populations reveals marked diversity in expression with critical roles in resolution of inflammation and airway immunity. *J. Immunol.* 189:2614–2624. http://dx.doi.org/10.4049/jimmunol.1200495

Gautier, E.L., T. Shay, J. Miller, M. Greter, C. Jakubzick, S. Ivanov, J. Helft, A. Chow, K.G. Elpek, S. Gordonov, et al; Immunological Genome Consortium. 2012b. Gene-expression profiles and transcriptional regulatory pathways that underlie the identity and diversity of mouse tissue macrophages. *Nat. Immunol.* 13:1118–1128. http://dx.doi.org/10.1038/ni.2419

Geissmann, F., S. Jung, and D.R. Littman. 2003. Blood monocytes consist of two principal subsets with distinct migratory properties. *Immunity.* 19:71–82. http://dx.doi.org/10.1016/S1074-7613(03)00174-2

Geissmann, F., M.G. Manz, S. Jung, M.H. Sieweke, M. Merad, and K. Ley. 2010. Development of monocytes, macrophages, and dendritic cells. *Science*. 327:656–661. http://dx.doi.org/10.1126/science.1178331

Ginhoux, F., M. Greter, M. Leboeuf, S. Nandi, P. See, S. Gokhan, M.F. Mehler, S.J. Conway, L.G. Ng, E.R. Stanley, et al. 2010. Fate mapping analysis reveals that adult microglia derive from primitive macrophages. *Science*. 330:841–845. http://dx.doi.org/10.1126/science.1194637

Godleski, J.J., and J.D. Brain. 1972. The origin of alveolar macrophages in mouse radiation chimeras. *J. Exp. Med.* 136:630–643. http://dx.doi.org/10.1084/jem.136.3.630

Golde, D.W. 1979. Alveolar proteinosis and the overfed macrophage. *Chest*. 76:119–120. http://dx.doi.org/10.1378/chest.76.2.119

Golde, D.W., M. Territo, T.N. Finley, and M.J. Cline. 1976. Defective lung macrophages in pulmonary alveolar proteinosis. *Ann. Intern. Med.* 85:304–309. http://dx.doi.org/10.7326/0003-4819-85-3-304

Gomez Perdiguero, E., C. Schulz, and F. Geissmann. 2013. Development and homeostasis of "resident" myeloid cells: The case of the microglia. *Glia*. 61:112–120. http://dx.doi.org/10.1002/glia.22393

Gonzalez-Rothi, R.J., and J.O. Harris. 1986. Pulmonary alveolar proteinosis. Further evaluation of abnormal alveolar macrophages. *Chest*. 90:656–661. http://dx.doi.org/10.1378/chest.90.5.656

Greter, M., J. Helft, A. Chow, D. Hashimoto, A. Mortha, J. Agudo-Cantero, M. Bogunovic, E.L. Gautier, J. Miller, M. Leboeuf, et al. 2012a. GM-CSF controls nonlymphoid tissue dendritic cell homeostasis but is dispensable for the differentiation of inflammatory dendritic cells. *Immunity*. 36:1031–1046. http://dx.doi.org/10.1016/j.immuni.2012.03.027

Greter, M., I. Lelios, P. Pelczar, G. Hoeffel, J. Price, M. Leboeuf, T.M. Kündig, K. Frei, F. Ginhoux, M. Merad, and B. Becher. 2012b. Stroma-derived interleukin-34 controls the development and maintenance of langerhans cells and the maintenance of microglia. *Immunity*. 37:1050–1060. http://dx.doi.org/10.1016/j.immuni.2012.11.001

Harris, J.O. 1979. Pulmonary alveolar proteinosis: abnormal in vitro function of alveolar macrophages. *Chest*. 76:156–159. http://dx.doi.org/10.1378/chest.76.2.156

Hashimoto, D., A. Chow, C. Noizat, P. Teo, M.B. Beasley, M. Leboeuf, C.D. Becker, P. See, J. Price, D. Lucas, et al. 2013. Tissue-resident macrophages self-maintain locally throughout adult life with minimal contribution from circulating monocytes. *Immunity*. 38:792–804. http://dx.doi.org/10.1016/j.immuni.2013.04.004

Hoeffel, G., Y. Wang, M. Greter, P. See, P. Teo, B. Malleret, M. Leboeuf, D. Low, G. Oller, F. Almeida, et al. 2012. Adult Langerhans cells derive predominantly from embryonic fetal liver monocytes with a minor contribution of yolk sac-derived macrophages. *J. Exp. Med.* 209:1167–1181. http://dx.doi.org/10.1084/jem.20120340

Huffman, J.A., W.M. Hull, G. Dranoff, R.C. Mulligan, and J.A. Whitsett. 1996. Pulmonary epithelial cell expression of GM-CSF corrects the alveolar proteinosis in GM-CSF-deficient mice. *J. Clin. Invest.* 97:649–655. http://dx.doi.org/10.1172/JCI118461

Kamath, A.T., S. Henri, F. Battye, D.F. Tough, and K. Shortman. 2002. Developmental kinetics and lifespan of dendritic cells in mouse lymphoid organs. *Blood*. 100:1734–1741.

Kennedy, D.W., and J.L. Abkowitz. 1997. Kinetics of central nervous system microglial and macrophage engraftment: analysis using a transgenic bone marrow transplantation model. *Blood*. 90:986–993.

Kennedy, D.W., and J.L. Abkowitz. 1998. Mature monocytic cells enter tissues and engraft. *Proc. Natl. Acad. Sci. USA*. 95:14944–14949. http://dx.doi.org/10.1073/pnas.95.25.14944

Lambrecht, B.N. 2006. Alveolar macrophage in the driver's seat. *Immunity*. 24:366–368. http://dx.doi.org/10.1016/j.immuni.2006.03.008

Landsman, L., and S. Jung. 2007. Lung macrophages serve as obligatory intermediate between blood monocytes and alveolar macrophages. *J. Immunol.* 179:3488–3494.

LeVine, A.M., J.A. Reed, K.E. Kurak, E. Cianciolo, and J.A. Whitsett. 1999. GM-CSF-deficient mice are susceptible to pulmonary group B streptococcal infection. *J. Clin. Invest.* 103:563–569. http://dx.doi.org/10.1172/JCI5212

Liu, K., C. Waskow, X. Liu, K. Yao, J. Hoh, and M. Nussenzweig. 2007. Origin of dendritic cells in peripheral lymphoid organs of mice. *Nat. Immunol.* 8:578–583. http://dx.doi.org/10.1038/ni1462

Misharin, A.V., L. Morales-Nebreda, G.M. Mutlu, G.R. Budinger, and H. Perlman. 2013. Flow Cytometric Analysis of the Macrophages and Dendritic Cell Subsets in the Mouse Lung. *Am. J. Respir. Cell Mol. Biol.* (Epub ahead of print).

Morrisey, E.E., and B.L. Hogan. 2010. Preparing for the first breath: genetic and cellular mechanisms in lung development. *Dev. Cell*. 18:8–23. http://dx.doi.org/10.1016/j.devcel.2009.12.010

Murphy, J., R. Summer, A.A. Wilson, D.N. Kotton, and A. Fine. 2008. The prolonged life-span of alveolar macrophages. *Am. J. Respir. Cell Mol. Biol.* 38:380–385. http://dx.doi.org/10.1165/rcmb.2007-0224RC

Nugent, K.M., and E.L. Pesanti. 1983. Macrophage function in pulmonary alveolar proteinosis. *Am. Rev. Respir. Dis.* 127:780–781.

Paine, R. III, S.B. Morris, H. Jin, S.E. Wilcoxen, S.M. Phare, B.B. Moore, M.J. Coffey, and G.B. Toews. 2001. Impaired functional activity of alveolar macrophages from GM-CSF-deficient mice. *Am. J. Physiol. Lung Cell. Mol. Physiol.* 281:L1210–L1218.

Plantinga, M., M. Guilliams, M. Vanheerswynghels, K. Deswarte, F. Branco-Madeira, W. Toussaint, L. Vanhoutte, K. Neyt, N. Killeen, B. Malissen, et al. 2013. Conventional and monocyte-derived CD11b(+) dendritic cells initiate and maintain T helper 2 cell-mediated immunity to house dust mite allergen. *Immunity*. 38:322–335. http://dx.doi.org/10.1016/j.immuni.2012.10.016

Reed, J.A., M. Ikegami, E.R. Cianciolo, W. Lu, P.S. Cho, W. Hull, A.H. Jobe, and J.A. Whitsett. 1999. Aerosolized GM-CSF ameliorates pulmonary alveolar proteinosis in GM-CSF-deficient mice. *Am. J. Physiol.* 276: L556–L563.

Reed, J.A., M. Ikegami, L. Robb, C.G. Begley, G. Ross, and J.A. Whitsett. 2000. Distinct changes in pulmonary surfactant homeostasis in common beta-chain- and GM-CSF-deficient mice. *Am. J. Physiol. Lung Cell. Mol. Physiol.* 278:L1164–L1171.

Schulz, C., E. Gomez Perdiguero, L. Chorro, H. Szabo-Rogers, N. Cagnard, K. Kierdorf, M. Prinz, B. Wu, S.E. Jacobsen, J.W. Pollard, et al. 2012. A lineage of myeloid cells independent of Myb and hematopoietic stem cells. *Science*. 336:86–90. http://dx.doi.org/10.1126/science.1219179

Serbina, N.V., and E.G. Pamer. 2006. Monocyte emigration from bone marrow during bacterial infection requires signals mediated by chemokine receptor CCR2. *Nat. Immunol.* 7:311–317. http://dx.doi.org/10.1038/ni1309

Shibata, Y., P.Y. Berclaz, Z.C. Chroneos, M. Yoshida, J.A. Whitsett, and B.C. Trapnell. 2001. GM-CSF regulates alveolar macrophage differentiation and innate immunity in the lung through PU.1. *Immunity*. 15:557–567. http://dx.doi.org/10.1016/S1074-7613(01)00218-7

Suzuki, T., T. Sakagami, B.K. Rubin, L.M. Nogee, R.E. Wood, S.L. Zimmerman, T. Smolarek, M.K. Dishop, S.E. Wert, J.A. Whitsett, et al. 2008. Familial pulmonary alveolar proteinosis caused by mutations in CSF2RA. *J. Exp. Med.* 205:2703–2710. http://dx.doi.org/10.1084/jem.20080990

Takahashi, K., F. Yamamura, and M. Naito. 1989. Differentiation, maturation, and proliferation of macrophages in the mouse yolk sac: a light-microscopic, enzyme-cytochemical, immunohistochemical, and ultrastructural study. *J. Leukoc. Biol.* 45:87–96.

Tamoutounour, S., S. Henri, H. Lelouard, B. de Bovis, C. de Haar, C.J. van der Woude, A.M. Woltman, Y. Reyal, D. Bonnet, D. Sichien, et al. 2012. CD64 distinguishes macrophages from dendritic cells in the gut and reveals the Th1-inducing role of mesenteric lymph node macrophages during colitis. *Eur. J. Immunol.* 42:3150–3166. http://dx.doi.org/10.1002/eji.201242847

Tarling, J.D., H.S. Lin, and S. Hsu. 1987. Self-renewal of pulmonary alveolar macrophages: evidence from radiation chimera studies. *J. Leukoc. Biol.* 42:443–446.

Thomassen, M.J., B.P. Barna, A.G. Malur, T.L. Bonfield, C.F. Farver, A. Malur, H. Dalrymple, M.S. Kavuru, and M. Febbraio. 2007. ABCG1 is deficient in alveolar macrophages of GM-CSF knockout mice and patients with pulmonary alveolar proteinosis. *J. Lipid Res.* 48:2762–2768. http://dx.doi.org/10.1194/jlr.P700022-JLR200

van Furth, R., and Z.A. Cohn. 1968. The origin and kinetics of mononuclear phagocytes. *J. Exp. Med.* 128:415–435. http://dx.doi.org/10.1084/jem.128.3.415

van oud Alblas, A.B., and R. van Furth. 1979. Origin, Kinetics, and characteristics of pulmonary macrophages in the normal steady state. *J. Exp. Med.* 149:1504–1518. http://dx.doi.org/10.1084/jem.149.6.1504

Varol, C., A. Vallon-Eberhard, E. Elinav, T. Aychek, Y. Shapira, H. Luche, H.J. Fehling, W.D. Hardt, G. Shakhar, and S. Jung. 2009. Intestinal lamina propria dendritic cell subsets have different origin and functions. *Immunity*. 31:502–512. http://dx.doi.org/10.1016/j.immuni.2009.06.025

Vermaelen, K., and R. Pauwels. 2004. Accurate and simple discrimination of mouse pulmonary dendritic cell and macrophage populations by flow cytometry: methodology and new insights. *Cytometry A*. 61:170–177. http://dx.doi.org/10.1002/cyto.a.20064

Virolainen, M. 1968. Hematopoietic origin of macrophages as studied by chromosome markers in mice. *J. Exp. Med*. 127:943–952. http://dx.doi.org/10.1084/jem.127.5.943

Wang, Y., K.J. Szretter, W. Vermi, S. Gilfillan, C. Rossini, M. Cella, A.D. Barrow, M.S. Diamond, and M. Colonna. 2012. IL-34 is a tissue-restricted ligand of CSF1R required for the development of Langerhans cells and microglia. *Nat. Immunol*. 13:753–760. http://dx.doi.org/10.1038/ni.2360

Willinger, T., A. Rongvaux, H. Takizawa, G.D. Yancopoulos, D.M. Valenzuela, A.J. Murphy, W. Auerbach, E.E. Eynon, S. Stevens, M.G. Manz, and R.A. Flavell. 2011. Human IL-3/GM-CSF knock-in mice support human alveolar macrophage development and human immune responses in the lung. *Proc. Natl. Acad. Sci. USA*. 108:2390–2395. http://dx.doi.org/10.1073/pnas.1019682108

Yamamoto, T., M. Naito, H. Moriyama, H. Umezu, H. Matsuo, H. Kiwada, and M. Arakawa. 1996. Repopulation of murine Kupffer cells after intravenous administration of liposome-encapsulated dichloromethylene diphosphonate. *Am. J. Pathol*. 149:1271–1286.

Yona, S., K.W. Kim, Y. Wolf, A. Mildner, D. Varol, M. Breker, D. Strauss-Ayali, S. Viukov, M. Guilliams, A. Misharin, et al. 2013. Fate mapping reveals origins and dynamics of monocytes and tissue macrophages under homeostasis. *Immunity*. 38:79–91. http://dx.doi.org/10.1016/j.immuni.2012.12.001

Yoshida, M., M. Ikegami, J.A. Reed, Z.C. Chroneos, and J.A. Whitsett. 2001. GM-CSF regulates protein and lipid catabolism by alveolar macrophages. *Am. J. Physiol. Lung Cell. Mol. Physiol*. 280:L379–L386.

Zsengellér, Z.K., J.A. Reed, C.J. Bachurski, A.M. LeVine, S. Forry-Schaudies, R. Hirsch, and J.A. Whitsett. 1998. Adenovirus-mediated granulocyte-macrophage colony-stimulating factor improves lung pathology of pulmonary alveolar proteinosis in granulocyte-macrophage colony-stimulating factor-deficient mice. *Hum. Gene Ther.* 9:2101–2109. http://dx.doi.org/10.1089/hum.1998.9.14-2101